Polymer Chemistry

ROYAL SOCIETY OF CHEMISTRY

PAPER

Cite this: *Polym. Chem.*, 2020, **11**, 6171

Facile synthesis and immobilization of boroxine polymers containing carbon chains and their application as adsorbents†

Nan Zhang,[a,b] Ying Su,[a,b] Yan Gao,[a,b] Tao Bao *[a,b] and Sicen Wang *[a,b]

Received 2nd June 2020,
Accepted 16th August 2020

DOI: 10.1039/d0py00797h

rsc.li/polymers

Boron-based covalent organic polymers are extremely popular adsorbents owing to their good adsorption properties. It is important and challenging to immobilize adsorbents on a substrate platform for their further application. In this study, boroxine-linked COPs (B-COPs) containing carbon chains were synthesized and immobilized on a microcap following a one-step solvent-thermal reaction. We used (3-aminopropyl)triethoxysilane to stabilize and catalyze the formation of boroxine rings, which also anchored B-COPs to the microcaps. To evaluate its adsorption property, the B-COP coated microcap (B-COPs@microcap) was subjected to novel stir bar sorptive extraction (SBSE) for separating the active anthraquinones from the complex matrices. Furthermore, the suspended B-COPs@microcap eliminated the mechanical abrasion of the adsorbed phase during the SBSE process. Highly sensitive detection of rhein and emodin was achieved with a low limit of detection (0.006 ng mL^{-1}) by coupling the bar sorptive extraction (BSE) with ultra-performance liquid chromatography (UPLC). The B-COPs@microcap exhibited good reproducibility, selectivity, and recyclability.

Introduction

Rhein and emodin are the main active anthraquinones in *Rheum palmatum* L., a traditional Chinese medicine (TCM).[1] They display various pharmacological effects, including anti-tumor, anti-bacterial, anti-inflammatory, and anti-oxidant properties.[2] Furthermore, rhein can ameliorate diabetic nephropathy, inhibit the formation of renal fibrosis, and protect organisms against kidney damage.[3,4] Emodin can lower the level of blood lipids, improve microcirculation, and treat acute liver injury.[5,6] Thus, the contents of rhein and emodin in biological fluids should be determined using an accurate and sensitive method, which could be further applied to study their pharmacokinetic parameters. High-performance liquid chromatography (HPLC) is an extensively used analytical method, which is often coupled with different detection techniques, such as ultraviolet and mass spectrometry. The detection limits of rhein and emodin can reach 3.85 ng mL^{-1} (ref. 7) and 0.3 ng mL^{-1},[1] respectively. For complex matrices and trace analytes' levels, the analytes should be separated and enriched by an adsorbent before analysis. Currently, ionic liquids,[8] natural deep eutectic solvents,[9,10] bis(tetraoxacalix[2]arene[2]triazine) modified silica gel,[11] dummy molecularly imprinted microspheres,[12] *etc.* have been utilized to extract rhein and emodin from plants, urine, and slimming tea. For fulfilling the increasing demands, adsorbents with high selectivity and adsorption capacity should be developed for the analysis of different analytes.

Covalent organic polymers (COPs) are a class of porous network materials built with C, H, O, N, and B through strong covalent bonds.[13,14] They have been extensively utilized for gas adsorption,[15] energy storage,[16] catalysis,[17] and biomedicine.[18] Moreover, COPs have also been exploited as adsorbents during sample preparation processes for separating and enriching targets from complex matrices. For example, Zhang's group fabricated a hydrazine-linked COP (HL-COP) and packed it in a stainless steel column for separating Sudan dyes from food samples.[19] Wang *et al.* synthesized a sulfonated hollow COP (sh-COP-P) to adsorb rhodamine B and methylene blue dyes in aqueous solution.[20] Also, Fu and co-workers proposed that sulfur-rich covalent triazine polymer nanospheres could efficiently remove Hg^{2+} from polluted water.[21] Among the different types of COPs, boron-based COPs are highly efficient owing to their reversible B–O bonds, which permits the formation of crystalline structures.[22–24] Currently, a series of crystalline boron-based COPs, such as COF-1 and COF-5, have been employed as adsorbed phases for magnetic solid-phase

[a]*School of Pharmacy, Health Science Center, Xi'an Jiaotong University, Xi'an710061, China. E-mail: baotao@xjtu.edu.cn, wangsc@mail.xjtu.edu.cn*
[b]*Shaanxi Engineering Research Center of Cardiovascular Drugs Screening & Analysis, Xi'an710061, China*

†Electronic supplementary information (ESI) available: Methods, Fig. S1–S8, and Tables S1–S4. See DOI: 10.1039/d0py00797h

extraction.[25,26] However, an electron-deficient boron atom is susceptible to nucleophilic attack. Boron-based COPs are easily degraded to monomers in a humid environment, which severely limits their application as adsorbents.[27,28] In 2011, Lavigne *et al.* reported that the hydrolytic stability of crystalline boronate ester-linked COPs can be enhanced by introducing alkyl chains.[29] Du and co-workers proved that crystalline boroxine-based COPs could be stabilized by (3-aminopropyl) triethoxysilane (APTES).[30] These strategies offered the inspiration for the synthesis and application of other boron-based COPs.

Immobilizing a material onto a substrate is an important and indispensable step for facilitating the separation of COPs from their matrices. Consequently, Liang *et al.* immobilized a triazine-imine COP on Fe_3O_4 nanoparticles for magnetic solid-phase extraction (MSPE) of pesticides in fruit samples.[31] Wang *et al.* fabricated hybrid melamine-based COP/ionic liquid monolithic columns to extract synthetic phenolic antioxidants from skincare products.[32] Yavuz's group reported the grafting of COPs on the surface of granular activated carbon for removing organic dyes and metals from water.[33] COPs have been incorporated into different supports and combined with diverse adsorption modes for extracting trace compounds from various samples. However, newer immobilization methods and adsorption modes should be further explored for separating different components of biological and commercial interest.

In this work, the monomer 9,9-dioctylfluorene-2,7-diboronic acid (DOFDB) was selected to fabricate boroxine-linked COPs (B-COPs) based on molecular self-condensation. A microcap was selected as a substrate for grafting B-COPs; this substrate has certain favorable characteristics, including small particle size, good mechanical strength, and active sites containing hydroxyl groups. Scheme 1a illustrates that the B-COPs containing carbon chains have been synthesized and immobilized on the surface of the microcap following a one-step method. Besides its usefulness as a network-stabilizer and catalyst,[30] APTES also functions as linking arms for the immobilization of B-COPs on the microcap. B-COPs containing carbon chains and phenyl rings can adsorb rhein and emodin *via* hydrophobic and π–π interactions. Besides, hydrogen bonding (O–H···O–B) and electrostatic interaction also play an important role in the selectivity of the adsorption. These interaction exist between $-B_3O_3$, –B–OH of B-COPs and –COOH, –OH of target molecules. Hence, the B-COP modified microcap (B-COPs@microcap) was utilized for the novel stir bar sorptive extraction (SBSE) of rhein and emodin from rat serum. SBSE has many advantages over other extraction techniques, such as good convenience and high adsorption capacity.[34] To eliminate the mechanical abrasion of the coating in the conventional SBSE mode, a suspended sorptive bar was developed. We named it bar sorptive extraction (BSE). The BSE mode (Scheme 1b) was employed by searing two grooves on the inner wall of a cone-shaped Teflon beaker. The B-COPs@microcap

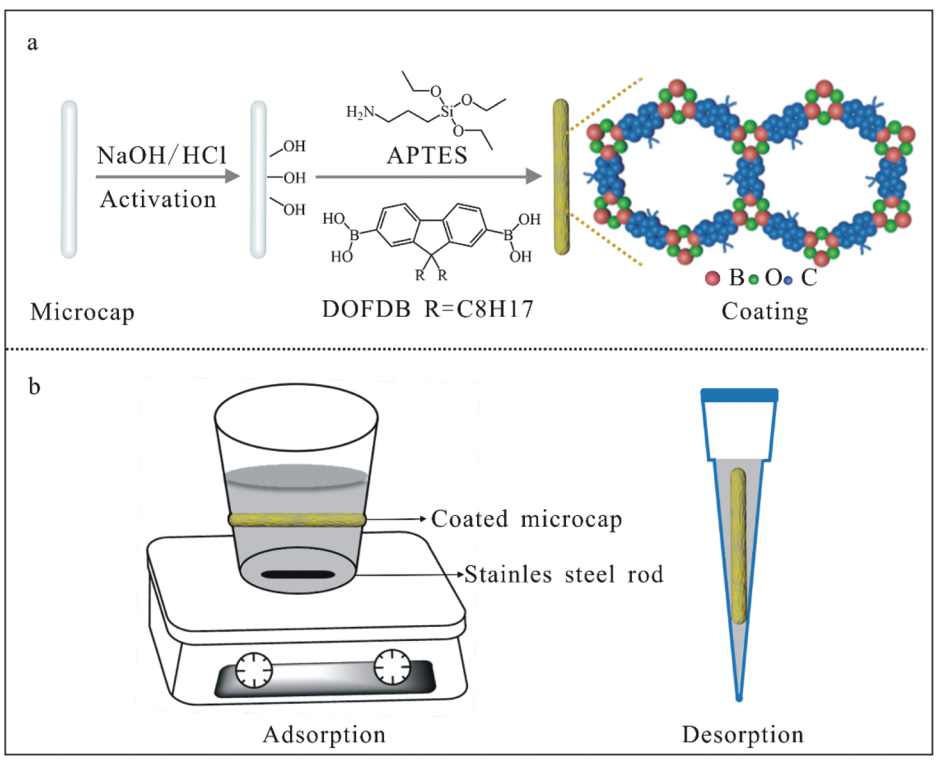

Scheme 1 Schematic diagrams of the immobilization process of the B-COPs@microcap (a) and the adsorption and desorption processes of BSE (b).

exhibited good reproducibility, stability, and recyclability. Several factors, including sample pH, extraction time, desorption solvent, and desorption time, which affect the adsorption capacity, were investigated. Under the optimized conditions, the B-COPs@microcap possessed high sensitivity and selectivity towards rhein and emodin.

Results and discussion

Synthesis and characterization

B-COPs were fabricated *via* the self-condensation of DOFDB. APTES was added to stabilize and catalyze the formation of B_3O_3 rings, which also anchored B-COPs to the microcap. The co-condensation of APTES and silanol groups on the surface of the microcap supplied amino groups (the necessary further modification). Then, the amino groups were linked to B-COPs *via* non-covalent interactions.[30] APTES and DOFDB were two important precursor compounds for preparing the B-COPs@microcap *via* a one-pot reaction. To improve the extraction capacity of the coating, the reaction temperature and the ratio and concentration of APTES and DOFDB were investigated individually. The results of the extraction under different preparation conditions are shown in Fig. S1 and S2.† The results show that the B-COP coated microcap, synthesized using 1.5 mg mL^{-1} of APTES and DOFDB at 95 °C, possesses a good adsorption property.

The surface of the bare microcap after modification with B-COPs displayed light yellow color. The morphology was further characterized by field emission scanning electron microscopy (FESEM). In Fig. 1, a (80-fold), b (5000-fold), and c (20 000-fold) are bare microcaps, and d (80-fold), e (5000-fold), and f (20 000-fold) are B-COPs@microcaps. Under high magnification, the surface of the bare microcap appeared relatively smooth, while after modification, many rough particulate matters were uniformly distributed on the surface of the microcap. The thickness of the B-COP coating is shown in Fig. S3,† which is estimated to be 378.9 nm.

The elemental analysis of B-COPs on the surface of the microcap was performed using an energy dispersive X-ray spectrometer (EDS). The results are shown in Fig. 2. Fig. 2A shows the elemental mapping images of the B-COP coated microcaps. In Fig. 2Aa, the green pane area has been selected for detection, exhibiting the characteristic elements of the B-COP coating, B element (Fig. 2Ab), C element (Fig. 2Ac), and N element (Fig. 2Ad). Fig. 2B shows the EDS spectrum with the atomic percentages of B, C, N, O, and Si. The elemental composition of the B-COP coating included B, C, and N. Large amounts of Si appeared because the microcap consisted of SiO_2. These results confirm the presence of B-COPs on the surface of the microcap after modification.

The structure of B-COPs has been confirmed by Fourier transform infrared spectroscopy (FT-IR). Fig. 3a shows the FT-IR spectrum of DOFDB (top) and B-COPs (bottom), which shows that the broad band at 3348.1 cm^{-1} was assigned to the O–H stretching vibration, and that the bands at 1357.5 cm^{-1} and 1326.8 cm^{-1} were related to the B–O stretching vibration. The bottom spectrum shows that the O–H stretching vibration has disappeared. The appearance of an out-of-plane deformation vibration of the boroxine ring at 710.6 cm^{-1} suggests that DOFDB has successfully self-condensed.[35]

The structure of B-COPs has been further studied by ^{13}C cross-polarization magic angle spinning (^{13}C CPMAS) and ^{11}B magic angle spinning (^{11}B MAS) nuclear magnetic resonance

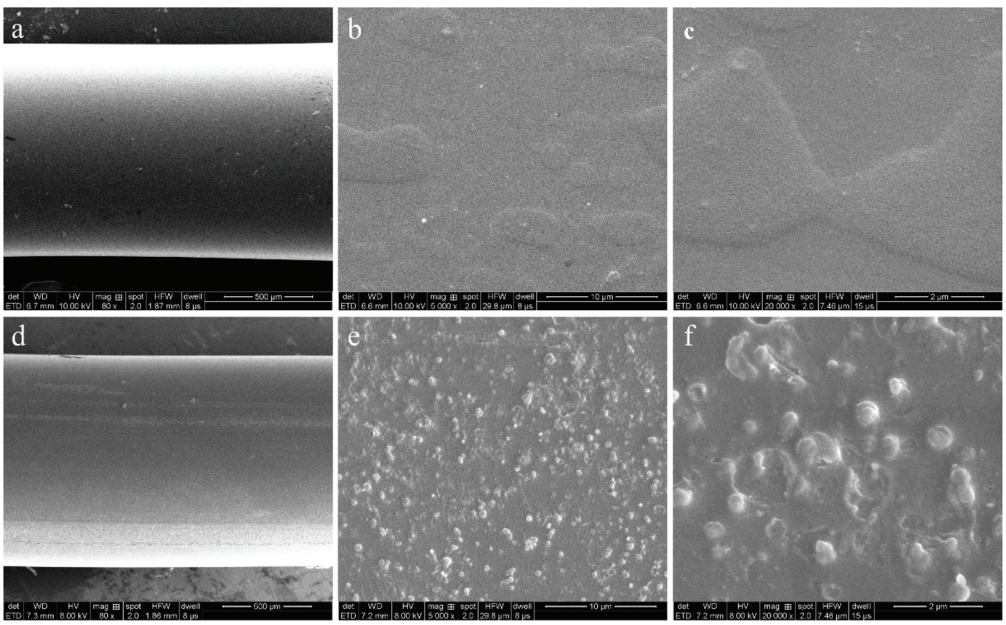

Fig. 1 FESEM images at 80-fold (a), 5000-fold (b), and 20 000-fold (c) of the bare microcap, and at 80-fold (d), 5000-fold (e), and 20 000-fold (f) of the B-COPs@microcap.

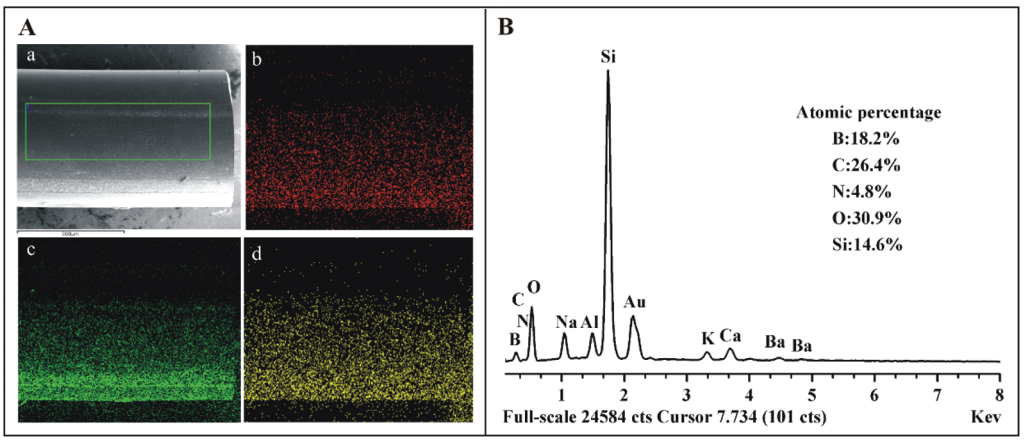

Fig. 2 (A) View area images (a) and EDS elemental mapping of B (b), C (c), and N (d); (B) EDS spectrum of the B-COP coated microcap.

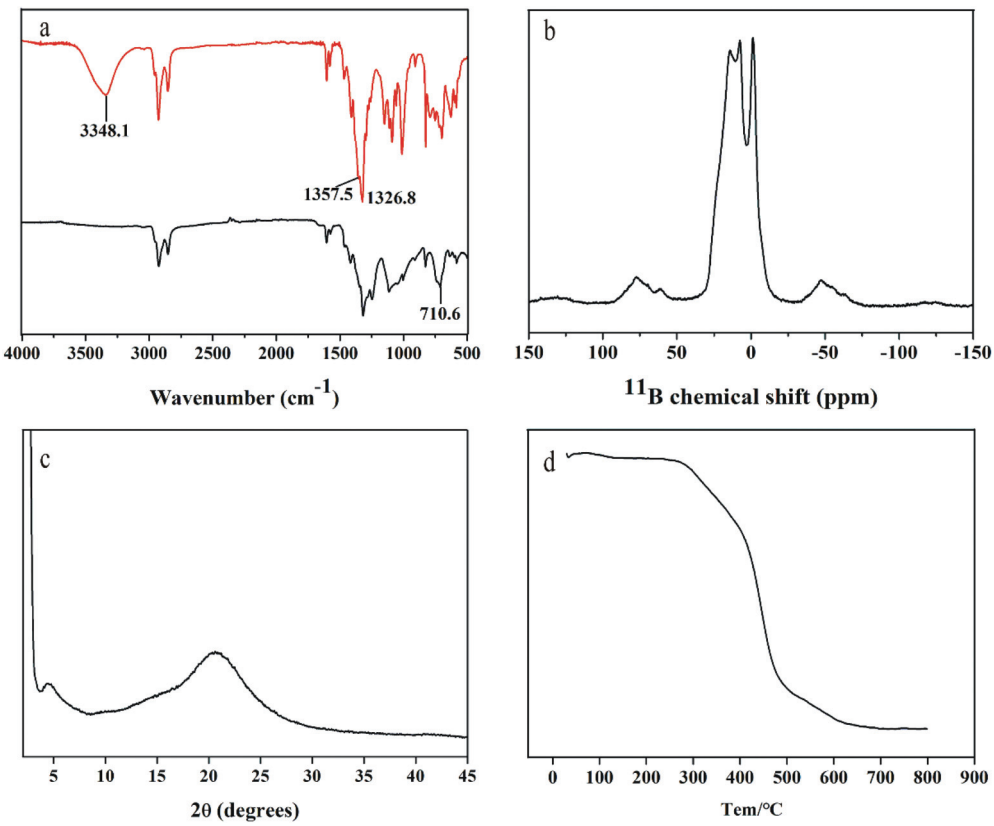

Fig. 3 (a) The FT-IR spectra of DOFDB (top) and B-COPs (bottom); (b) the ^{11}B NMR spectra of B-COPs; (c) the XRD pattern of B-COPs; (d) the TG curve of B-COPs.

(NMR) spectroscopy. The spectrum of ^{13}C CPMAS is shown in Fig. S4.† The peak at 120.7 ppm is assigned to C-B_3O_3. Fig. 3b shows the tricoordinate boron (B[3]) and tetrahedral-coordinated boron (B[4]) species. The resonance at −1.3 ppm is assigned to B[4], which demonstrates the Brønsted-type and Lewis-type interactions with the amine groups of APTES. The B[3] peaks at 7.4 ppm and 14.5 ppm are attributed to the boroxine backbone.[30,36]

The structure of B-COPs has been confirmed using an X-ray diffractometer (XRD). Fig. 3c shows the diffraction pattern of B-COP powder, and the data have been collected in the range of 2θ = 2–45° with 1° min^{-1}. The XRD pattern shows broad diffraction peaks at approximately 2θ of 4.3°, 20°, and 41°, which indicates that the structure of B-COPs has a poor crystal order. Thus, it has been named B-COPs, a kind of boroxine polymer.

The thermal properties of B-COPs were evaluated using thermogravimetric (TG) analysis. The TG curve was scanned from room temperature to 800 °C at a heating rate of 10 °C min^{-1} under N_2 ambiance. According to Fig. 3d, the material suffered 0.45% weight loss before 285.2 °C and 5.40% weight loss before 307.2 °C, and then diminished sharply with the increase in temperature. The results indicate that B-COPs are thermally stable at 285.2 °C.

The porosity of B-COPs was investigated by the nitrogen adsorption/desorption experiment at 77 K. According to Fig. S5,† the Brunauer–Emmett–Teller (BET) surface area is not high (8.71 m^2 g^{-1}) because the inner space of the material is occupied by carbon chains.[37] The pore size was calculated using the quenched solid density functional theory (QSDFT) model. The dominant pore size has been located at 1.83 nm (Fig. S6†), indicating the presence of micropores.

Adsorption study of rhein and emodin

The B-COPs@microcap was used in BSE for separating the active anthraquinones from the complex matrices to evaluate its adsorption behavior. To obtain high extraction efficiency, several factors, including sample pH, extraction time, desorption solvent, and desorption time, were investigated. The results are shown in Fig. 4. About 20 mL of the sample solution, containing emodin (13 ng ml^{-1}) and rhein (18 ng mL^{-1}), was prepared by diluting the stock solution with deionized water.

Effect of pH. The effect of the pH value on the extraction efficiency, ranging from 4.5 to 8.5, was studied. Fig. 4a shows that the peak area increases greatly from 4.5 to 5.5 and decreases slowly from 5.5 to 8.5. Rhein (pK_a = 4.51, 8.41) and emodin (pK_a = 5.70, 7.92) contain phenolic hydroxyl groups, and rhein possesses a carboxyl group. The pH value affects the existing form of the compound. Rhein and emodin exist in protonated or neutral forms at pH < pK_a and in deprotonated forms at pH > pK_a. Moreover, the pH value also affects the electrostatic charge on the coating of boronic acid groups. When the pH values of the solutions varied from 4.5 to 5.5, the coating was positively charged, and the analytes existed in the deprotonated or neutral forms; therefore, the electrostatic attraction increased. When the pH values were increased from 5.5 to 8.5, most of the analytes existed in the deprotonated form; meanwhile, the coating was negatively charged. An increase in electrostatic repulsion reduced the extraction efficiency. The existing forms of rhein and emodin at pH 5.5 benefited the adsorption efficiency of the B-COP coating. Thus, the pH value of the sample solution was adjusted to 5.5 with 0.1 M HCl before BSE.

Effect of the extraction time. The extraction time would influence the transport of analytes from the matrix to adsorbed phase, which was investigated from 30 to 90 min. In Fig. 4b, the peak area increased continuously within 30–75 min. It remained almost constant with a further increase to 90 min because the adsorption equilibrium was reached at 75 min. Therefore, 75 min was selected as the extraction time for further studies.

Effect of desorption solvent. A suitable solvent is essential for the desorption of the targets. Several desorption solvents, including ethanol, ethanol–water (v/v, 1/1), ethyl acetate, acetone, and aqueous sodium carbonate solution, were investigated. The eluting ability of the sodium carbonate solution for

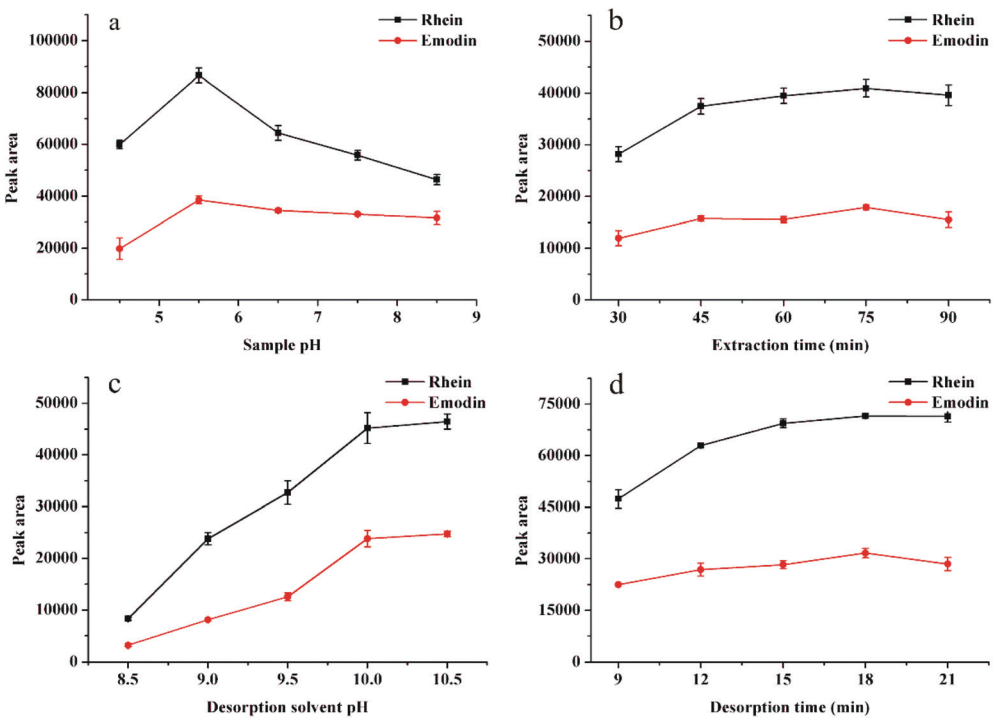

Fig. 4 The effect of pH (a), extraction time (b), pH of the desorption solvent (c), and desorption time (d) on the extraction efficiency. Conditions: sample volume, 20 mL; concentration of analytes, 13 ng mL^{-1} of emodin and 18 ng mL^{-1} of rhein; stirring rate, 1100 rpm; volume of the desorption solvent, 200 μL.

rhein and emodin was much better than those of other solvents. The coating was negatively charged, and the analytes transformed into the deprotonated state under weak basic conditions, enhancing the hydrophilic effect and electrostatic repulsion interaction. Then, the pH of the aqueous solution was further optimized. In Fig. 4c, the result shows that the peak area increased significantly when the pH was varied from 8.5 to 10.0, and then it increased slightly from 10.0 to 10.5. The analytes were further deprotonated when the pH was increased. The surface of the coating exhibited negative charge owing to the deprotonation reaction of boronic acid groups. Thus, the electrostatic repulsion became stronger, and most of the analytes entered the solution phase. To prevent the damage of the high pH value on the stability of the coating, sodium carbonate solution (pH value at 10.0) was selected as the desorption solvent.

Effect of the desorption time. The effect of the desorption time, ranging from 9 to 21 min, was tested on the extraction efficiency. In Fig. 4d, the result shows that the peak area increased in the range of 9 to 18 min, and that it remained almost constant after 18 min because the desorption process reached equilibrium. Thus, 18 min was selected as the desorption time.

Adsorption capacity. Under the optimal extraction conditions, the extraction capacity of the B-COPs@microcap was evaluated by increasing the concentration of rhein and emodin in a stepwise manner. The adsorption amount *versus* analyte concentration curve was plotted. Fig. S7† shows that the adsorption amount increased in the range of 0.1–250 ng mL^{-1} for rhein and 0.1–150 ng mL^{-1} for emodin. Then, it almost remained stable after 250 ng mL^{-1} and 150 ng mL^{-1} because adsorption saturation was reached. Therefore, the adsorption capacity with one coated microcap was estimated to be 1.17 μg for rhein and 0.45 μg for emodin.

Preparation reproducibility and recyclability of the B-COPs@microcap

The preparation reproducibility of the B-COPs@microcap was investigated. Seven bars from the same batch and seven bars from different batches were employed to extract rhein and emodin from aqueous solutions. The results are presented in Table 1. The preparation reproducibility of the intra-batch and inter-batch ranged from 3.1% to 3.6% and 5.0% to 7.0%, respectively.

The recyclability of the B-COPs@microcap was evaluated by repeatedly extracting rhein and emodin. In Table S1,† the results show that RSDs are less than 7.5% in the 10-time repeat, revealing that the coating is stable and recyclable.

Table 1 The preparation reproducibility (RSD, %) of the B-COPs@microcap for the determination of emodin (c = 13 ng mL^{-1}) and rhein (c = 18 ng mL^{-1})

Analytes	Bar to bar (n = 7)	Batch to batch (n = 7)
Rhein	3.1%	5.0%
Emodin	3.6%	7.0%

Analytical performance

The analytical method for determining rhein and emodin by BSE coupling using ultra-performance liquid chromatography (UPLC) was validated under the optimal extraction conditions. The analytical results are presented in Table S2.† The limits of detection (LODs) for rhein and emodin were 0.015 ng mL^{-1} and 0.006 ng mL^{-1}, respectively, and the limits of quantification (LOQs) were 0.045 ng mL^{-1} and 0.018 ng mL^{-1}, respectively. The correlation coefficients (R^2) were more than 0.9990 in the concentration range of 0.1–50 ng mL^{-1}. The repeatability was determined using seven parallel analyses of the standard aqueous solution (20 mL) containing each target at 10 ng mL^{-1}, and the RSD was 4.5% for rhein and 5.9% for emodin. The absolute enrichment efficiency of the coated microcap was calculated by the ratio of the adsorption amount of the targets with BSE and the initial amount in the sample solution; the equation was $EE = (C_{ds} \times V_{ds})/(C_{ss} \times V_{ss}) \times 100\%$, where C_{ds}, C_{ss}, V_{ds} and V_{ss} are the concentrations of analytes in the desorption solvent, concentrations of analytes in the sample solution, volume of the desorption solvent, and volume of the sample solution, respectively; the EE value was 54.4% for rhein and 39.5% for emodin.

Adsorption in complex matrices

The applicability of the developed method in a complex sample was examined. Blank plasma was collected from healthy adult male Sprague-Dawley rats and treated by protein removal. Then, the treated sample was used as the loading solution and analyzed by the B-COPs@microcap-BSE-UPLC method. The typical chromatograms of the direct injection, spiked standards before and after extraction using the proposed method are shown in Fig. S8.† After extraction, rhein and emodin were determined with good peak shapes without the interference of the matrix after spiking the standard. The accuracy of the proposed method was validated. The recoveries of the spiked serum sample solution with standards at 0.5 ng mL^{-1}, 5 ng mL^{-1}, and 20 ng mL^{-1} are listed in Table S3.† Good recoveries were obtained in the range of 85%–106%. The results show that this method can be applied to monitor trace levels of rhein and emodin in complex matrices. In Table S4,† the proposed method has been compared to other reported methods. The results demonstrate that B-COPs-BSE-UPLC has good application potential for the highly selective and sensitive analysis of rhein and emodin in complex samples, with a wide linear range.

Conclusions

In this work, a new B-COP containing carbon chain was synthesized and utilized as a sorbent in BSE. The B-COPs were immobilized on the surface of a microcap by a one-step solvent-thermal reaction. The successful formation of B-COPs

on the microcap was confirmed by FESEM, EDS, FT-IR, NMR, and XRD. The fabricated B-COPS@microcap was locked by the grooves of a Teflon beaker to eliminate mechanical abrasion. Combined with UPLC, the B-COPs@microcap exhibited high selectivity towards rhein and emodin.

Animal ethics statement

All animals were bred and maintained in a pathogen-free environment at the Animal Experimental Center of Xi'an Jiaotong University. All animal procedures were conducted in accordance with the Guidelines for the Care and Use of Laboratory Animals of Xi'an Jiaotong University and approved by the Animal Ethics Committee of Xi'an Jiaotong University.

Conflicts of interest

The authors declare no conflicts of interest.

Acknowledgements

This work was supported by the National Natural Science Foundation of China (Grant No. 81703469 and 81973277), the World-Class Universities (Disciplines), the Characteristic Development Guidance Funds for the Central Universities (No. PY3A012), and the Fundamental Research Funds for the Central Universities.

Notes and references

1 H. Zhu, X. Liu, T. T. Zhu, X. L. Wang, K. M. Qin, K. Pei and B. C. Cai, *J. Sep. Sci.*, 2017, **40**, 2382–2389.
2 S. A. Pandith, R. A. Dar, S. K. Lattoo, M. A. Shah and Z. A. Reshi, *Phytochem. Rev.*, 2018, **17**, 573–609.
3 G. Wang, Q. Li, D. Chen, B. Wu, Y. Wu, W. Tong and P. Huang, *Theranostics*, 2019, **9**, 6191–6208.
4 H. Sun, G. W. Luo, Z. Xiang, X. J. Cai and D. H. Chen, *Phytomedicine*, 2016, **23**, 1661–1670.
5 R. Xie, M. Liu and S. Li, *Artif. Cells, Nanomed., Biotechnol.*, 2019, **47**, 1877–1887.
6 Y. Ding, P. Liu, Z. L. Chen, S. J. Zhang, Y. Q. Wang, X. Cai, L. Luo, X. Zhou and L. Zhao, *Front. Pharmacol.*, 2018, **9**, 962.
7 A. Arvindekar, G. R. Pereira and K. S. Laddha, *J. Food Sci. Technol.*, 2015, **52**, 6574–6582.
8 Y. Fan, Z. Niu, C. Xu, L. Yang and T. Yang, *Molecules*, 2019, **24**, 2770.
9 Y. C. Wu, P. Wu, Y. B. Li, T. C. Liu, L. Zhang and Y. H. Zhou, *RSC Adv.*, 2018, **8**, 15069–15077.
10 W. W. Deng, Y. Zong and Y. X. Xiao, *ACS Sustainable Chem. Eng.*, 2017, **5**, 4267–4427.
11 K. Hu, Y. Qiao, Z. Deng, M. Wu and W. Liu, *J. Anal. Methods Chem.*, 2017, **2017**, 1–10.
12 X. Wu, S. Liang, X. Ge, Y. Lv and H. Sun, *J. Sep. Sci.*, 2015, **38**, 1263–1270.
13 N. Chaoui, M. Trunk, R. Dawson, J. Schmidt and A. Thomas, *Chem. Soc. Rev.*, 2017, **46**, 3302–3321.
14 C. Li, P. Li, L. Chen, M. E. Briggs and S. Ren, *J. Polym. Sci., Part A: Polym. Chem.*, 2017, **55**, 2383–2389.
15 Y. Cui, J. Du, Y. Liu, Y. Yu, S. Wang, H. Pang, Z. Liang and J. Yu, *Polym. Chem.*, 2018, **9**, 2643–2649.
16 B. C. Patra, S. Khilari, L. Satyanarayana, D. Pradhan and A. Bhaumik, *Chem. Commun.*, 2016, **52**, 7592–7595.
17 B. C. Patra, S. Khilari, R. N. Manna, S. Mondal and A. Bhaumik, *ACS Catal.*, 2017, **7**, 6120–6127.
18 H. Wang, W. Zhu, L. Feng, Q. Chen, Y. Chao, Z. Dong and Z. Liu, *Nano Res.*, 2017, **11**, 1–14.
19 C. Zhang, G. Li and Z. Zhang, *J. Chromatogr. A*, 2015, **1419**, 1–9.
20 J. Wang, Y. Zhang, L. An, W. Wang, Y. Zhang and X. Bu, *Chin. J. Chem.*, 2018, **36**, 826–830.
21 Y. Fu, W. Yu, W. Zhang, Q. Huang, J. Yan, C. Pan and G. Yu, *Polym. Chem.*, 2018, **9**, 4125–4131.
22 J. M. Winne, L. Leibler and F. Du Prez, *Polym. Chem.*, 2019, **10**, 6091–6108.
23 P. Chakma and D. Konkolewicz, *Angew. Chem., Int. Ed.*, 2019, **58**, 9682–9695.
24 Z. P. Zhang, M. Z. Rong and M. Q. Zhang, *Prog. Polym. Sci.*, 2018, **80**, 39–93.
25 Y. Chen and Z. Chen, *Talanta*, 2017, **165**, 188–193.
26 J. Wang, J. Li, M. Gao and X. Zhang, *Nanoscale*, 2017, **9**, 10750–10756.
27 C. R. Deblase and W. R. Dichtel, *Macromolecules*, 2016, **49**, 5297–5305.
28 H. Li, H. Li, Q. Dai, H. Li and J.-L. Bredas, *Adv. Theory Simul.*, 2018, **1**, 1700015.
29 L. M. Lanni, R. W. Tilford, M. Bharathy and J. J. Lavigne, *J. Am. Chem. Soc.*, 2011, **133**, 13975–13983.
30 Y. Du, D. C. Calabro, B. Wooler, P. Kortunov, Q. Li, S. M. Cundy and K. Mao, *Chem. Mater.*, 2015, **27**, 1445–1447.
31 R. Liang, Y. Peng, Y. Hu and G. Li, *J. Sep. Sci.*, 2019, **42**, 1432–1439.
32 H. Wang, H. Zhang, S. Wei and Q. Jia, *J. Chromatogr. A*, 2018, **1566**, 23–31.
33 P. D. Mines, D. Thirion, B. Uthuppu, Y. Hwang, M. H. Jakobsen, H. R. Andersen and C. T. Yavuz, *Chem. Eng. J.*, 2017, **309**, 766–771.
34 F. A. Hansen and S. Pedersen-Bjergaard, *Anal. Chem.*, 2020, **92**, 2–15.
35 A. P. Cote, A. I. Benin, N. W. Ockwig, M. O'Keeffe, A. J. Matzger and O. M. Yaghi, *Science*, 2005, **310**, 1166–1170.
36 Y. T. Angel Wong and D. L. Bryce, *Annu. Rep. NMR Spectrosc.*, 2018, **93**, 213–279.
37 G. Zhang, Y.-l. Hong, Y. Nishiyama, S. Bai, S. Kitagawa and S. Horike, *J. Am. Chem. Soc.*, 2019, **141**, 1227–1234.